Combining multiband remote sensing and hierarchical distance sampling to establish drivers of bird abundance

Ronny Richter [1, 2, 3, *, #], Arend Heim [1, #], Wieland Heim [4], Johannes Kamp [4] and Michael Vohland [1, 2]

[1] Geoinformatics and Remote Sensing, Institute for Geography, Leipzig University, Johannisallee 19a, 04103 Leipzig, Germany
[2] German Centre for Integrative Biodiversity Research (iDiv) Halle-Jena-Leipzig, Deutscher Platz 5e, 04103 Leipzig, Germany
[3] Systematic Botany and Functional Biodiversity, Institute for Biology, Leipzig University, Johannisallee 21, 04103 Leipzig, Germany
[4] Institute of Landscape Ecology, University of Mu̇nster, Heisenbergstraße 2, 48149 Mu̇nster, Germany

* Correspondence: ronny.richter@idiv.de
# joined first authorship

Supplementary Materials:

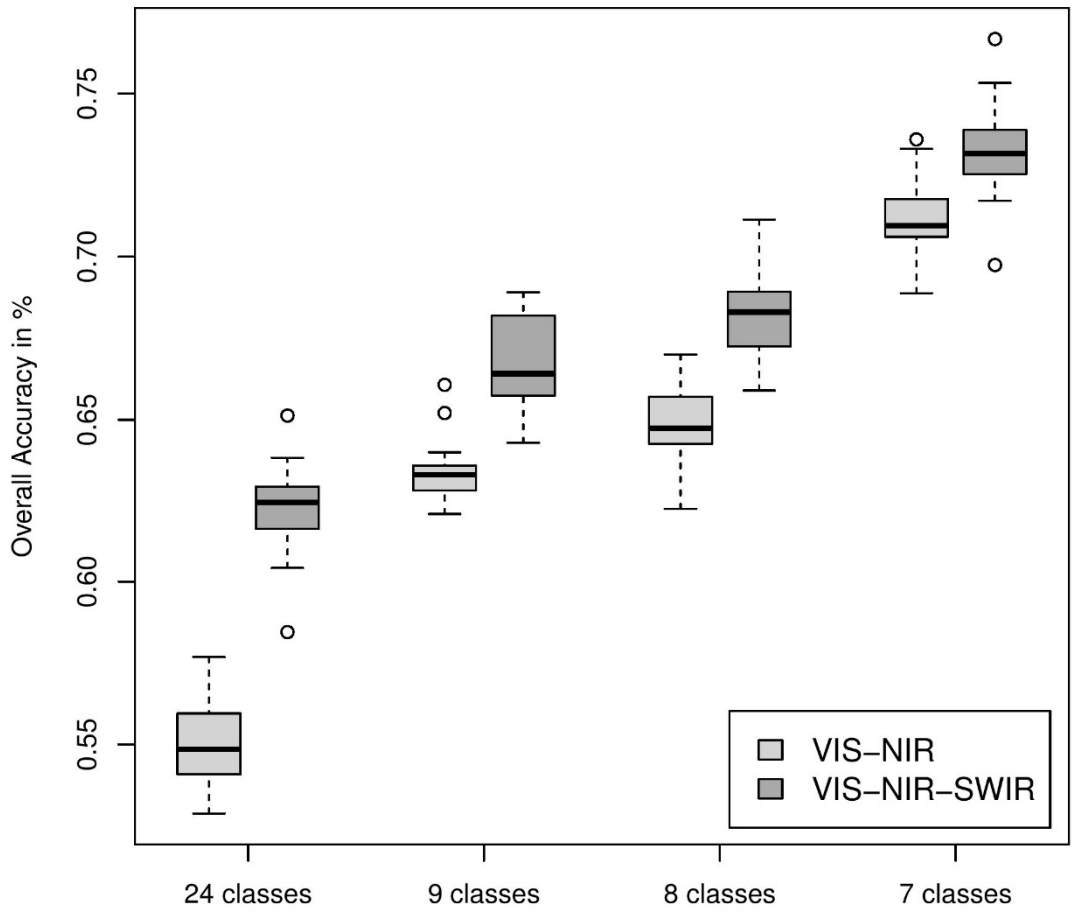

Figure 1. Achieved overall accuracies for the classification of different aggregation levels for land cover classes, VIS-NIR (SPOT6) compared to the multi-band VIS-NIR-SWIR product.

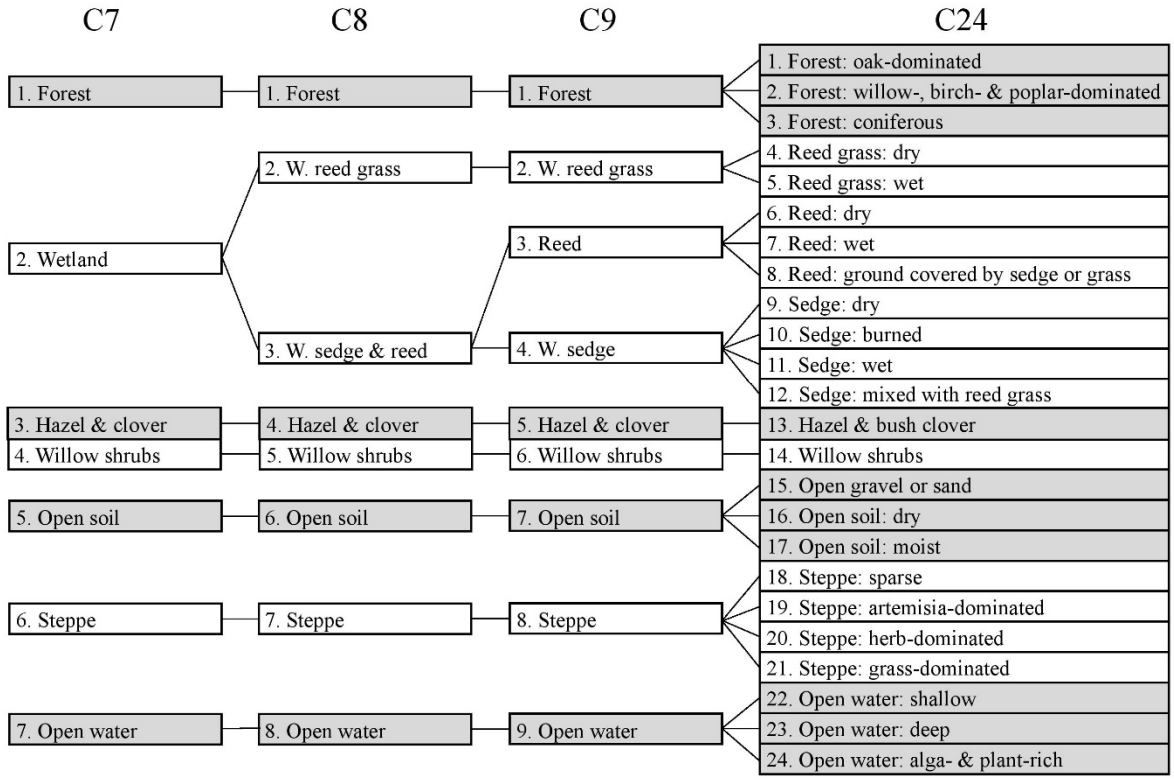

Figure 2. Scheme explaining the aggregation of land cover types used for the mapping with remote sensing data.

Tables 1. AIC values as achieved in model selection. The model resulting in the lowest AIC value was chosen as the final model. Models with negative relationships for land cover type on bird species abundance were not considered and are thus grayed out.

Yellow-breasted Bunting

Model	Nr. of parameters	AIC
λ(willow) φ(repetition) σ(–) α	7	623.2
λ(–) φ(repetition) σ(–) α	6	625.7
λ(–) φ(repetition + time) σ(–) α	7	631.1
λ(forest) φ(–) σ(–) α	5	664.1
λ(forest^2) φ(–) σ(–) α	5	674.5
λ(–) φ(time) σ(–) α	5	675.1
λ(hazel & clover) φ(–) σ(–) α	5	678.6
λ(shannon^2) φ(–) σ(–) α	5	679.5
λ(willow) φ(–) σ(–) α	5	679.9
λ(willow^2) φ(–) σ(–) α	5	679.9
λ(steppe) φ(–) σ(–) α	5	680.5
λ(steppe^2) φ(–) σ(–) α	5	681.5
λ(–) φ(–) σ(–) α	4	682.2
λ(hazel & clover^2) φ(–) σ(–) α	5	682.2
λ(wetland) φ(–) σ(–) α	5	682.6
λ(water^2) φ(–) σ(–) α	5	683.0
λ(water) φ(–) σ(–) α	5	683.3
λ(wetland^2) φ(–) σ(–) α	5	683.5
λ(open soil) φ(–) σ(–) α	5	684.1
λ(shannon) φ(–) σ(–) α	5	684.2
λ(open soil^2) φ(–) σ(–) α	5	684.2
λ(–) φ(–) σ(–)	3	721.3

Ochre-rumped Bunting

Model	Nr. of parameters	AIC
λ(forest) φ(–) σ(–) α	5	663.1
λ(forest²) φ(–) σ(–) α	5	670.0
λ(hazel & clover) φ(–) σ(–) α	5	671.3
λ(wetland) φ(–) σ(observer) α	6	671.6
λ(hazel & clover ²) φ(–) σ(–) α	5	672.0
λ(shannon²) φ(–) σ(–) α	5	672.5
λ(–) φ(–) σ(observer) α	5	673.8
λ(wetland) φ(–) σ(–) α	5	673.9
λ(O) φ(–) σ(–) α	5	674.1
λ(wetland) φ(repetition) σ(–) α	8	674.2
λ(wetland) φ(repetition) σ(observer) α	8	674.2
λ(–) φ(repetition) σ(–) α	6	674.8
λ(–) φ(–) σ(–) α	4	676.0
λ(shannon) φ(–) σ(–) α	5	676.4
λ(steppe) φ(–) σ(–) α	5	676.6
λ(–) φ(repetition + time) σ(–) α	7	676.8
λ(open soil²) φ(–) σ(–) α	5	677.0
λ(willow²) φ(–) σ(–) α	5	677.0
λ(willow) φ(–) σ(–) α	5	677.3
λ(–) φ(time) σ(–) α	5	677.4
λ(wetland²) φ(–) σ(–) α	5	677.4
λ(water²) φ(–) σ(–) α	5	677.4
λ(water) φ(–) σ(–) α	5	677.8
λ(steppe²) φ(–) σ(–) α	5	678.0
λ(–) φ(–) σ(–)	3	726.1

Black-faced Bunting

Model	Nr. of parameters	AIC
λ(shannon) φ(–) σ(observer) α	6	971.0
λ(–) φ(–) σ(observer) α	5	975.4
λ(shannon) φ(–) σ(–) α	5	975.5
λ(willow²) φ(–) σ(–) α	5	977.1
λ(shannon²) φ(–) σ(–) α	5	978.8
λ(–) φ(–) σ(–) α	4	979.7
λ(wetland) φ(–) σ(–) α	5	979.8
λ(wetland²) φ(–) σ(–) α	5	980.0
λ(–) φ(time) σ(–) α	5	980.1
λ(water) φ(–) σ(–) α	5	980.3
λ(water²) φ(–) σ(–) α	5	980.4
λ(forest) φ(–) σ(–) α	5	980.6
λ(willow) φ(–) σ(–) α	5	981.0
λ(open soil²) φ(–) σ(–) α	5	981.0
λ(hazel & clover) φ(–) σ(–) α	5	981.1
λ(open soil) φ(–) σ(–) α	5	981.1
λ(steppe) φ(–) σ(–) α	5	981.3
λ(steppe²) φ(–) σ(–) α	5	981.5
λ(hazel & clover²) φ(–) σ(–) α	5	981.6
λ(forest²) φ(–) σ(–) α	5	981.7
λ(–) φ(repetition) σ(–) α	6	982.2
λ(–) φ(repetition + time) σ(–) α	7	982.7
λ(–) φ(–) σ(–)	3	984.8